



VIBRATION AND BUCKLING OF COMPOSITE THIN-WALLED BEAMS WITH SHEAR DEFORMABILITY

V. H. CORTÍNEZ AND M. T. PIOVAN

Grupo de Análisis de Sistemas Mecánicos, Facultad Regional Bahía Blanca, Universidad Tecnológica Nacional (FRBB), 11 de Abril 461, 8000, Bahía Blanca, Argentina. E-mail: vcortine@frbb.utn.edu.ar

(Received 21 January 2000, and in final form 1 February 2002)

In this paper, a theoretical model is developed for the dynamic analysis of composite thin-walled beams with open or closed cross-sections. The present model incorporates, in a full form, the shear flexibility (bending and warping shear) as well as a state of initial stresses. This allows to study the free vibration and buckling problems in a unified fashion. An analytical solution of the developed equations is obtained for the case of simply supported thin-walled beams. Numerical examples are given to demonstrate the importance of the shear flexibility on the vibration and buckling behavior of the considered structures.

© 2002 Elsevier Science Ltd. All rights reserved.

1. INTRODUCTION

Structural members made of composites are increasingly used in aeronautical, mechanical and civil engineering applications where high strength and stiffness, and low weight are of primary importance. Other advantages that motivate some applications are corrosion resistance, enhanced fatigue life, low thermal expansion, etc. [1]. Many structural members made of composites have the form of thin-walled beams. Accordingly, a significant amount of research has been conducted in recent years toward the development of theoretical and computational methods for analyzing the structural behavior of such members.

The structural analysis of isotropic thin-walled open beams is appropriately performed by means of Vlasov's theory. This theory considers the warping effect that is of great importance in this type of structures [2]. Vlasov's theory was extended to composites by Bauld and Tzeng [3]. Recently, Ghorbanpoor and Omidvar [4] introduced new equivalent moduli of elasticity and rigidity to allow decoupling (in an approximate form) of the Bauld and Tzeng equations. In this way, the composite thin-walled open beam is treated by means of Vlasov's theory with new equivalent moduli of elasticity. This simplified approach yields practically the same numerical values as those by Bauld and Tzeng's model. Massa and Barbero proposed a strength of materials formulation for static analysis of composite thin-walled beams [5]. A study about the determination of the shear center in composite beams was carried out by Pollok *et al.* [6]. In the case of box beams made of orthotropic materials and subjected to tension and bending, Estivalezes and Barrau [7] developed a simplified method to calculate stresses and strains.

However, the above-mentioned works do not consider the influence of the shear flexibility on the dynamics of the member. This effect is important for predicting the

dynamic behavior of thin-walled open beams made of isotropic materials, as shown by Cortínez *et al.* [8–10]. For the case of composite thin-walled beams, the shear effect may be even more important owing to the high value of the ratio between the longitudinal elasticity modulus and the transverse elasticity modulus. Sherbourne and Kabir [11] analyzed the shear effect in connection with the lateral stability of composite I-section beams. Godoy *et al.* [12] developed a mathematical model for I-section composite beams considering shear effects and cross-sectional distortion for interactive buckling analysis. Shear flexibility associated to bending and new formulas for the shear coefficients were analyzed by Omidvar [13]. The static behavior of tailored composite box-beams considering only bending shear was performed by Smith and Chopra [14]. Song and Librescu [15] developed a theory for the dynamic analysis of anisotropic composite thin-walled closed beams. This model takes into account the shear flexibility due to bending displacements in addition to primary and secondary warping effects. These authors presented interesting applications and extensions of this last theory [16–18].

None of the papers cited above have considered the shear flexibility due to warping. This effect may be very important in several situations. Moreover, taking into account the coupled dynamic behavior of thin-walled members due to both cross-sectional geometry and laminate characteristics, warping shear may also affect the dominant flexural modes.

According to the authors' knowledge, the only study taking into account the shear flexibility, in a full form, is that of Wu and Sun [19]. However, in their paper, emphasis was given in showing the effectiveness of the developed finite element and not in characterizing the shear effect on the dynamics of the member. Moreover, initial stresses were not considered.

In this paper, a theoretical model is presented for the dynamic analysis of composite, open and closed cross-sectional, thin-walled beams with initial stresses. This model takes into account, in a full form, the shear flexibility (bending and warping shear). On the other hand, it is strictly valid for symmetric balanced laminates and especially orthotropic laminates [1]. The present equations are obtained by means of a Hellinger–Reissner formulation of composite shells.

The model is used for analyzing the free vibration and buckling problems in a unified fashion. To do this, an analytical solution of the present equations is performed for the case of simply supported thin-walled beams. Parametric analyses are done to evaluate the influence of the shear flexibility as well as the effect of the initial stresses on the natural frequencies and buckling loads of beams with different cross-sectional shapes and laminate architecture.

2. THEORY

2.1. ASSUMPTIONS

A composite thin-walled beam with an arbitrary cross-section is considered (Figure 1). The points of the structural member are referred to a Cartesian co-ordinate system (x, \bar{y}, \bar{z}) , where the x -axis is parallel to the longitudinal axis of the beam while \bar{y} and \bar{z} are the principal axes of the cross-section. The axes y, z are parallel to the principal ones but having their origin at the shear center (defined according to Vlasov's theory of isotropic beams). The co-ordinates corresponding to points lying on the middle line are denoted as Y and Z (or \bar{Y} and \bar{Z}). In addition, a circumferential co-ordinate s and a normal co-ordinate n are introduced on the middle contour of the cross-section. On the other hand, y_0 and z_0 are the centroidal co-ordinates measured with respect to the shear center.

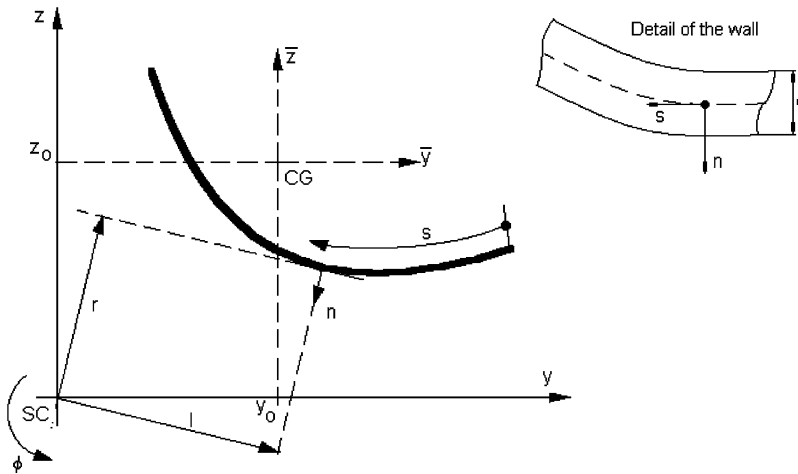


Figure 1. Co-ordinate system of the cross-section.

The present structural model is based on the following assumptions: (1) the cross-section contour is rigid in its own plane; (2) the warping distribution is assumed to be given by the Saint–Venant function for isotropic beams; (3) shell force and moment resultants corresponding to the circumferential stress σ_{ss} and the force resultant corresponding to γ_{ns} are neglected; (4) the radius of curvature at any point of the shell is neglected; (5) twisting curvature of the shell is expressed according to the classical plate theory, but bending curvature is expressed according to the first order shear deformation theory; in fact, bending shear strain of the wall is incorporated; (6) initial shell force and initial bending moment resultants, N_{xx}^0 and M_{xx}^0 related to σ_{xx}^0 are taken into account and (7) the laminate stacking sequence is assumed to be symmetric and balanced, or specially orthotropic [1] (the corresponding constitutive equations for the shell stress resultants are given in Appendix A).

2.2. VARIATIONAL FORMULATION

Taking into account the adopted assumptions, the Hellinger–Reissner principle for a composite shell may be expressed in the form [20]

$$\begin{aligned}
 & \iint (N_{xx} \delta \varepsilon_{xx}^L + M_{xx} \delta \kappa_{xx}^L + N_{xs} \delta \gamma_{xs}^L + M_{xs} \delta \kappa_{xs}^L + N_{xn} \delta \gamma_{xn}^L + N_{xx}^0 \delta \varepsilon_{xx}^{NL} + M_{xx}^0 \delta \kappa_{xx}^{NL}) ds dx \\
 & + \iint \left[e \rho \left(\frac{\partial^2 \bar{U}}{\partial t^2} \delta \bar{U} + \frac{\partial^2 \bar{V}}{\partial t^2} \delta \bar{V} + \frac{\partial^2 \bar{W}}{\partial t^2} \delta \bar{W} \right) + \frac{e^3 \rho}{12} \left(\frac{\partial^2 \phi_x}{\partial t^2} \delta \phi_x + \frac{\partial^2 \phi_s}{\partial t^2} \delta \phi_s \right) \right] ds dx \\
 & - \iint [\bar{q}_x \delta \bar{U} + \bar{q}_s \delta \bar{V} + \bar{q}_n \delta \bar{W} + \bar{m}_x \delta \phi_x + \bar{m}_s \delta \phi_s] ds dx \\
 & - \left[\int (\bar{N}_{xx} \delta \bar{U} + \bar{M}_{xx} \delta \phi_x + \bar{N}_{xs} \delta \bar{V} + \bar{M}_{xs} \delta \phi_s + \bar{N}_{xn} \delta \bar{W}) ds \right]_{x=0}^{x=L} = 0, \tag{1a}
 \end{aligned}$$

$$\begin{aligned}
 & \iint \left[\left(\varepsilon_{xx}^L - \frac{N_{xx}}{A_{11}} \right) \delta N_{xx} + \left(\gamma_{xs}^L - \frac{N_{xs}}{A_{66}} \right) \delta N_{xs} + \left(\kappa_{xs}^L - \frac{M_{xs}}{D_{66}} \right) \delta M_{xs} \right] ds dx \\
 & + \iint \left[\left(\kappa_{xx}^L - \frac{M_{xx}}{D_{11}} \right) \delta M_{xx} + \left(\gamma_{xn}^L - \frac{N_{xn}}{A_{55}^{(H)}} \right) \delta N_{xn} \right] ds dx = 0, \tag{1b}
 \end{aligned}$$

where N_{xx} , N_{xs} , M_{xx} , M_{xs} and N_{xn} are shell stress resultants defined according to the following expressions:

$$N_{xx} = \int_{-e/2}^{e/2} \sigma_{xx} \, dn, \quad M_{xx} = \int_{-e/2}^{e/2} (\sigma_{xx}n) \, dn, \quad M_{xs} = \int_{-e/2}^{e/2} (\sigma_{xs}n) \, dn, \quad (2a-c)$$

$$N_{xs} = \int_{-e/2}^{e/2} \sigma_{xs} \, dn, \quad N_{xn} = \int_{-e/2}^{e/2} \sigma_{xn} \, dn. \quad (2d, e)$$

Initial shell stress resultants are denoted with the superscript “ \bullet^0 ” and the applied shell stress resultants on the boundaries are denoted as “ \bullet ”. \bar{q}_x , \bar{q}_s and \bar{q}_n are applied forces per unit area in the directions x , s and n , respectively, while \bar{m}_x and \bar{m}_s are applied couples per unit area about the directions s and x respectively. On the other hand, the shell strains are defined in the form

$$\varepsilon_{xx}^L = \frac{\partial \bar{U}}{\partial x}, \quad \kappa_{xx}^L = -\frac{\partial \phi_x}{\partial x}, \quad \gamma_{xs}^L = \frac{\partial \bar{U}}{\partial s} + \frac{\partial \bar{V}}{\partial x}, \quad \kappa_{xs}^L = -2\frac{\partial^2 \bar{W}}{\partial x \partial s}, \quad (3a-d)$$

$$\gamma_{xn}^L = \frac{\partial \bar{W}}{\partial x} - \phi_x, \quad \varepsilon_{xx}^{NL} = \frac{1}{2} \left[\left(\frac{\partial \bar{V}}{\partial x} \right)^2 + \left(\frac{\partial \bar{W}}{\partial x} \right)^2 \right], \quad (3e, f)$$

$$\kappa_{xx}^{NL} = \frac{\partial \phi_s}{\partial x} \frac{\partial \bar{V}}{\partial x}, \quad (3g)$$

where \bar{U} , \bar{V} and \bar{W} are the shell displacements in the x , s and n directions, respectively, whereas ϕ_x and ϕ_s are bending rotations about s and x respectively.

It should be noted that, in equations (1), the stress resultants and the displacements are variationally independent quantities. Expressions (1a) and (1b) represent the variational forms of the dynamic equilibrium and constitutive equations respectively.

2.3. KINEMATIC EXPRESSIONS

The displacement field [8] (compatible with assumptions 1 and 2) are assumed to be expressed in the form

$$u_x = u_0(x) - \theta_z(x)\bar{y}(s, n) - \theta_y(x)\bar{z}(s, n) + \theta(x)\omega(s, n), \quad (4a)$$

$$u_y = v(x) - \phi(x)z(s, n), \quad u_z = w(x) + \phi(x)y(s, n), \quad (4b, c)$$

where

$$\bar{y}(s, n) = y(s, n) - y_0, \quad \bar{z}(s, n) = z(s, n) - z_0, \quad (5a, b)$$

$$\bar{y}(s, n) = \bar{Y}(s) - n \frac{dZ}{ds}, \quad \bar{z}(s, n) = \bar{Z}(s) + n \frac{dY}{ds}, \quad (5c, d)$$

$$y(s, n) = Y(s) - n \frac{dZ}{ds}, \quad z(s, n) = Z(s) + n \frac{dY}{ds}. \quad (5e, f)$$

The warping function ω of the thin-walled cross-section may be defined as

$$\omega = \omega_p(s) + \omega_s(s, n), \quad (6)$$

where ω_p and ω_s are the contour warping function and the thickness warping function respectively. They are defined in the form [8,14]

$$\omega_p(s) = \frac{1}{S} \left[\int_0^S \left(\int_{s_0}^s [r(s) - \psi(s)] ds \right) ds \right] - \int_{s_0}^s [r(s) - \psi(s)] ds, \quad \omega_s(s, n) = -nl(s), \quad (7a, b)$$

where

$$r(s) = -Z(s) \frac{dY}{ds} + Y(s) \frac{dZ}{ds}, \quad l(s) = Y(s) \frac{dY}{ds} + Z(s) \frac{dZ}{ds}. \quad (8a, b)$$

In expression (7), ψ is the shear strain in the middle line, obtained by means of the Saint–Venant theory of pure torsion for isotropic beams, and normalized with respect to $d\phi/dx$ [21]. For the case of open sections $\psi = 0$.

The displacements with respect to the curvilinear system (x, s, n) are obtained by means of the following expressions:

$$\bar{U} = u_x(x, s, 0), \quad \bar{V} = u_y(x, s, 0) \frac{dY}{ds} + u_2(x, s, 0) \frac{dZ}{ds}, \quad (9a, b)$$

$$\bar{W} = -u_y(x, s, 0) \frac{dZ}{ds} + u_2(x, s, 0) \frac{dY}{ds}, \quad \phi_x = -\frac{\partial u_x}{\partial n}, \quad (9c, d)$$

$$\phi_s = \frac{\partial}{\partial n} \left(u_y \frac{dY}{ds} + u_2 \frac{dZ}{ds} \right). \quad (9e)$$

Substituting shell displacements (9) into strain definitions (3) one obtains

$$\epsilon_{xx}^L = u'_0 - \theta'_z Y(s) - \theta'_y Z(s) + \theta' \omega_p(s), \quad (10a)$$

$$\kappa_{xx}^L = \theta'_z \frac{dZ}{ds} - \theta'_y \frac{dY}{ds} - \theta' l(s), \quad (10b)$$

$$\gamma_{xs}^L = (v' - \theta_z) \frac{dY}{ds} + (w' - \theta_y) \frac{dZ}{ds} + (\phi' - \theta)(r - \psi) + \psi \phi', \quad (10c)$$

$$\kappa_{xs}^L = -2\phi', \quad \gamma_{xn}^L = -(v' - \theta_z) \frac{dZ}{ds} + (w' - \theta_y) \frac{dY}{ds} + (\phi' - \theta)l(s), \quad (10d, e)$$

$$\epsilon_{xx}^{NL} = \frac{1}{2} [(v'^2 + w'^2) + \phi'^2 (r^2 + l^2)] + \phi' \left[v' \left(r(s) \frac{dY}{ds} - l(s) \frac{dZ}{ds} \right) + w' \left(r(s) \frac{dZ}{ds} + l(s) \frac{dY}{ds} \right) \right], \quad (10f)$$

$$\kappa_{xx}^{NL} = -[\phi'^2 r] - \phi' \left[v' \left(\frac{dY}{ds} \right) + w' \left(\frac{dZ}{ds} \right) \right]. \quad (10g)$$

In the above expressions $(\bullet)'$ denotes derivation with respect to the variable x .

The first and second terms of expressions (10c) and (10e) may be considered as the shear strains associated to bending, the third term corresponds to the warping shear and the last term in expression (10c) is the Saint–Venant (pure torsion) shear strain.

2.4. EQUATIONS OF MOTION

Substituting expressions (9) and (10) into equation (1a) and integrating with respect to s , one obtains the one-dimensional expression for the virtual work equation given by

$$L_K + L_{KG} + L_M + L_P = 0, \quad (11)$$

where

$$L_K = \int_0^L (N\delta u'_0 - M_z\delta\theta'_z - M_y\delta\theta'_y + B\delta\theta' + Q_y\delta(v' - \theta_z) + Q_z\delta(w' - \theta_y) + T_w\delta(\phi' - \theta) + T_{sv}\delta\phi') dx, \tag{12a}$$

$$L_{KG} = \int_0^L \left\{ \frac{N^0}{2} \delta \left[(w')^2 + (v')^2 + \frac{I_S}{A} (\phi')^2 + 2y_0(\phi'w') - 2z_0(\phi'v') \right] + \frac{M_z^0}{2} \delta [\beta_z(\phi')^2 + 2\phi'w'] + \frac{M_y^0}{2} \delta [\beta_y(\phi')^2 - 2\phi'v'] + \frac{B^0}{2} \delta [\beta_w(\phi')^2] \right\} dx, \tag{12b}$$

$$L_M = \int_0^L \bar{\rho} \left[A \frac{\partial^2 u_0}{\partial t^2} \delta u_0 + I_z \frac{\partial^2 \theta_z}{\partial t^2} \delta \theta_z + I_y \frac{\partial^2 \theta_y}{\partial t^2} \delta \theta_y + C_w \frac{\partial^2 \theta}{\partial t^2} \delta \theta + A \frac{\partial^2}{\partial t^2} (v - z_0\phi) \delta v + A \frac{\partial^2}{\partial t^2} (w + y_0\phi) \delta w + \frac{\partial^2}{\partial t^2} (-Az_0v + Ay_0w + I_S\phi) \delta \phi \right] dx, \tag{12c}$$

$$L_P = \int_0^L (-q_x\delta u_0 - q_y\delta v - q_z\delta w + m_z\delta\theta_z + m_y\delta\theta_y - b\delta\theta - m_x\delta\phi) dx + [\bar{N}\delta u_0 - \bar{M}_z\delta\theta_z - \bar{M}_y\delta\theta_y + \bar{B}\delta\theta + \bar{Q}_y\delta v + \bar{Q}_z\delta w + (\bar{T}_w + \bar{T}_{sv})\delta\phi]_{x=0}^{x=L}. \tag{12d}$$

In the previous equations, the following definitions, for the beam forces, have been made:

$$N = \int_S N_{xx} ds, \quad M_Y = \int_S \left(N_{xx}\bar{Z} + M_{xx} \frac{dY}{ds} \right) ds, \tag{13a, b}$$

$$M_Z = \int_S \left(N_{xx}\bar{Y} - M_{xx} \frac{dZ}{ds} \right) ds, \quad B = \int_S (N_{xx}\omega_p + M_{xx}l(s)) ds, \tag{13c, d}$$

$$Q_Y = \int_S \left(N_{xs} \frac{dY}{ds} - N_{xn} \frac{dZ}{ds} \right) ds, \quad Q_Z = \int_S \left(N_{xs} \frac{dZ}{ds} + N_{xn} \frac{dY}{ds} \right) ds, \tag{13e, f}$$

$$T_W = \int_S [N_{xs}(r - \psi) + N_{xn}l(s)] ds, \quad T_{SV} = \int_S (N_{xs}\psi - 2M_{xs}) ds. \tag{13g, h}$$

In the above expressions the integration is carried out over the middle contour perimeter. N is the axial force, M_Z, M_Y are the bending moments, B is the bimoment, Q_Y, Q_Z are the shear forces, T_W is the flexural-torsional moment and T_{SV} is the Saint-Venant torsional moment, N^0, M_z^0, M_y^0, B^0 are the initial forces, $\bar{N}, \bar{M}_y, \bar{M}_z, \bar{B}, \bar{Q}_y, \bar{Q}_z, \bar{T}_w, \bar{T}_{sv}$ correspond to external generalized forces acting at the ends, q_x, q_y and q_z are the applied forces per unit length in the directions x, y and z , respectively, while m_x, m_y and m_z are the applied couples per unit length about the directions x, y and z , respectively, and b is the applied bimoment per unit length. A is the cross-sectional area, I_Z and I_Y are the principal moments of inertia of the cross-section, C_W is the warping constant, I_S is the polar moment with respect to the shear center and $\bar{\rho}$ is the mean density of the laminate.

Also, the following coefficients have been defined:

$$\beta_z = \frac{1}{I_z} \int_S \left[\bar{Y}(Y^2 + Z^2)e - r(s) \frac{e^3}{6} \frac{dY}{ds} \right] ds, \tag{14a}$$

$$\beta_y = \frac{1}{I_y} \int_S \left[\bar{Z}(Y^2 + Z^2)e + r(s) \frac{e^3}{6} \frac{dZ}{ds} \right] ds, \tag{14b}$$

$$\beta_\omega = \frac{1}{C_w} \int_S \left[\omega_P (Y^2 + Z^2) e + r(s) \frac{e^3}{6} I(s) \right] ds. \quad (14c)$$

One may notice that L_K, L_{KG}, L_M and L_P represent the virtual work contributions due to the incremental, initial, inertial and external forces respectively. In reference [8], equations (11) and (12) were obtained for the case of isotropic beams. This may be explained considering the fact that the virtual work equation holds irrespective of the constitutive equations of the material.

Taking variations with respect to the generalized displacements $u_0, \theta_z, v, \theta_y, w, \theta$ and ϕ , as indicated in equations (12), one obtains the following equations of motion:

$$-\frac{\partial N}{\partial x} + \bar{\rho} A \frac{\partial^2 u_0}{\partial t^2} = q_x, \quad (15a)$$

$$\frac{\partial M_z}{\partial x} - Q_y + \bar{\rho} I_z \frac{\partial^2 \theta_z}{\partial t^2} = -m_z, \quad (15b)$$

$$-\frac{\partial Q_y}{\partial x} + \bar{\rho} A \frac{\partial^2 (v - z_0 \phi)}{\partial t^2} - \frac{\partial}{\partial x} \left(N^0 \frac{\partial v}{\partial x} \right) + \frac{\partial}{\partial x} \left[(M_y^0 + N^0 z_0) \frac{\partial \phi}{\partial x} \right] = q_y, \quad (15c)$$

$$\frac{\partial M_y}{\partial x} - Q_z + \bar{\rho} I_y \frac{\partial^2 \theta_y}{\partial t^2} = -m_y, \quad (15d)$$

$$-\frac{\partial Q_z}{\partial x} + \bar{\rho} A \frac{\partial^2 (w + y_0 \phi)}{\partial t^2} - \frac{\partial}{\partial x} \left(N^0 \frac{\partial w}{\partial x} \right) - \frac{\partial}{\partial x} \left[(M_z^0 + N^0 y_0) \frac{\partial \phi}{\partial x} \right] = q_z, \quad (15e)$$

$$-\frac{\partial B}{\partial x} - T_w + \bar{\rho} C_w \frac{\partial^2 \theta}{\partial t^2} = b, \quad (15f)$$

$$\begin{aligned} & -\frac{\partial (T_w + T_{sv})}{\partial x} + \bar{\rho} A \frac{\partial^2}{\partial t^2} \left(\frac{I_S}{A} \phi - z_0 v + y_0 w \right) + \frac{\partial}{\partial x} \left[N^0 \left(-\frac{I_S}{A} \frac{\partial \phi}{\partial x} - y_0 \frac{\partial w}{\partial x} + z_0 \frac{\partial v}{\partial x} \right) \right] \\ & - \frac{\partial}{\partial x} \left[(M_z^0 \beta_z + M_y^0 \beta_y + B^0 \beta_w) \frac{\partial \phi}{\partial x} \right] - \frac{\partial}{\partial x} \left(M_z^0 \frac{\partial w}{\partial x} \right) + \frac{\partial}{\partial x} \left(M_y^0 \frac{\partial v}{\partial x} \right) = m_x, \end{aligned} \quad (15g)$$

subjected to the following boundary conditions (at $x = 0, L$):

$$N - \bar{N} = 0 \quad \text{or} \quad \delta u_0 = 0, \quad (16a)$$

$$-M_z + \bar{M}_z = 0 \quad \text{or} \quad \delta \theta_z = 0, \quad (16b)$$

$$Q_y + N^0 \frac{\partial v}{\partial x} + (M_y^0 - N^0 z_0) \frac{\partial \phi}{\partial x} - \bar{Q}_y = 0 \quad \text{or} \quad \delta v = 0, \quad (16c)$$

$$-M_y + \bar{M}_y = 0 \quad \text{or} \quad \delta \theta_y = 0, \quad (16d)$$

$$Q_z + N^0 \frac{\partial w}{\partial x} + (M_z^0 + N^0 y_0) \frac{\partial \phi}{\partial x} - \bar{Q}_z = 0 \quad \text{or} \quad \delta w = 0, \quad (16e)$$

$$B - \bar{B} = 0 \quad \text{or} \quad \delta \theta = 0, \quad (16f)$$

$$\begin{aligned} & (T_w + T_{sv}) + N^0 \left(\frac{I_S}{A} \frac{\partial \phi}{\partial x} + y_0 \frac{\partial w}{\partial x} - z_0 \frac{\partial v}{\partial x} \right) + M_z^0 \left(\beta_z \frac{\partial \phi}{\partial x} + \frac{\partial w}{\partial x} \right) \\ & + M_y^0 \left(\beta_y \frac{\partial \phi}{\partial x} - \frac{\partial v}{\partial x} \right) + B^0 \beta_w \frac{\partial \phi}{\partial x} - (\bar{T}_w + \bar{T}_{sv}) = 0 \quad \text{or} \quad \delta \phi = 0. \end{aligned} \quad (16g)$$

In these equations, the terms corresponding to the initial stresses contributions have been underlined.

2.5. CONSTITUTIVE EQUATIONS FOR THE BEAM STRESS RESULTANTS

The field of the shell stress resultants is assumed to be of the form

$$N_{xx} = e \left[\frac{N}{A} + \frac{M_y}{I_y} \bar{Z} + \frac{M_z}{I_z} \bar{Y} + \frac{B}{C_w} \omega_P \right], \quad (17a)$$

$$M_{xx} = \frac{e^3}{12} \left[\frac{M_y}{I_y} \frac{dY}{ds} - \frac{M_z}{I_z} \frac{dZ}{ds} - \frac{B}{C_w} l(s) \right], \quad (17b)$$

$$M_{xs} = -\frac{e^3}{6J} T_{SV}, \quad (17c)$$

$$N_{xs} = e \left[-\frac{Q_Z}{I_y} \bar{\lambda}_y(s) - \frac{Q_Y}{I_z} \bar{\lambda}_z(s) + \frac{T_W}{C_w} \bar{\lambda}_\omega(s) \right] + \frac{e\psi(s)}{J} T_{SV}, \quad (17d)$$

$$N_{xn} = \frac{e^3}{12} \left[\frac{Q_Z}{I_y} \frac{dY}{ds} - \frac{Q_Y}{I_z} \frac{dZ}{ds} - \frac{T_W}{C_w} l(s) \right]. \quad (17e)$$

In expressions (17c) and (17d), J denotes the Saint–Venant torsion constant. In expression (17d), $\bar{\lambda}_y, \bar{\lambda}_z$ and $\bar{\lambda}_\omega$ are defined as

$$\bar{\lambda}_y(s) = \int_0^s \bar{Z}(s) ds + \frac{\alpha}{S} \oint \left[\int_0^s \bar{Z}(s) ds \right] ds, \quad (18a)$$

$$\bar{\lambda}_z(s) = \int_0^s \bar{Y}(s) ds + \frac{\alpha}{S} \oint \left[\int_0^s \bar{Y}(s) ds \right] ds, \quad (18b)$$

$$\bar{\lambda}_\omega(s) = \int_0^s \omega_P(s) ds + \frac{\alpha}{S} \oint \left[\int_0^s \omega_P(s) ds \right] ds, \quad (18c)$$

where $\alpha = 0$ or 1 depending on whether the cross-section contour is open or closed respectively. S denotes the contour perimeter.

The selected field of shell stress resultants (17) verifies expressions (13) in addition to the following shell equilibrium equations:

$$\frac{\partial N_{xx}}{\partial x} + \frac{\partial N_{xs}}{\partial s} = 0, \quad \frac{\partial M_{xx}}{\partial x} + \frac{\partial M_{xs}}{\partial s} - N_{xn} = 0. \quad (19a, b)$$

Substituting expressions (17) into equation (1b), integrating with respect to “ s ” and taking variations with respect to $N, M_y, M_z, B, Q_y, Q_z, T_w$ and T_{sv} , one obtains the following constitutive equations for the beam stress resultants:

$$N = E^* A \frac{\partial u_0}{\partial x}, \quad M_z = -E^* I_z \frac{\partial \theta_z}{\partial x}, \quad M_y = -E^* I_y \frac{\partial \theta_y}{\partial x}, \quad (20a-c)$$

$$B = E^* C_w \frac{\partial \theta}{\partial x}, \quad T_{SV} = G^{**} J \frac{\partial \phi}{\partial x}, \quad (20d, e)$$

$$\begin{Bmatrix} Q_y \\ Q_z \\ T_w \end{Bmatrix} = G^* [S] \begin{Bmatrix} \frac{\partial v}{\partial x} - \theta_z \\ \frac{\partial w}{\partial x} - \theta_y \\ \frac{\partial \phi}{\partial x} - \theta \end{Bmatrix}, \tag{20f}$$

where E^* , G^* and G^{**} are expressed in the form

$$E^* = \frac{\bar{A}_{11}}{e}, \quad G^* = \frac{\bar{A}_{66}}{e}, \tag{21a, b}$$

$$G^{**} = \begin{cases} G^* & \text{for closed sections,} \\ \frac{12\bar{D}_{66}}{e^3} & \text{for open sections.} \end{cases} \tag{21c}$$

The S -matrix arising in equation (20f) is obtained as

$$[S] = \begin{bmatrix} \int_S \left(\frac{\bar{\lambda}_z}{I_z}\right)^2 A_{yy}^{(n)} ds & \int_S \frac{\bar{\lambda}_z \bar{\lambda}_y A_{yz}^{(n)}}{I_z I_y} ds & - \int_S \frac{\bar{\lambda}_z \bar{\lambda}_\omega A_{y\omega}^{(n)}}{I_z C_w} ds \\ \int_S \frac{\bar{\lambda}_z \bar{\lambda}_y A_{yz}^{(n)}}{I_z I_y} ds & \int_S \left(\frac{\bar{\lambda}_y}{I_y}\right)^2 A_{zz}^{(n)} ds & - \int_S \frac{\bar{\lambda}_\omega \bar{\lambda}_y A_{z\omega}^{(n)}}{C_w I_y} ds \\ - \int_S \frac{\bar{\lambda}_z \bar{\lambda}_\omega A_{y\omega}^{(n)}}{I_z C_w} ds & - \int_S \frac{\bar{\lambda}_\omega \bar{\lambda}_y A_{z\omega}^{(n)}}{C_w I_y} ds & \int_S \left(\frac{\bar{\lambda}_\omega}{C_w}\right)^2 A_{\omega\omega}^{(n)} ds \end{bmatrix}^{-1}. \tag{22}$$

In expression (22), the following definitions have been introduced:

$$A_{yy}^{(n)} = 1 + \frac{e^4 \bar{A}_{66}}{144 \bar{A}_{55}^{(H)}} \frac{\int_S \left(\frac{dZ}{ds}\right)^2 ds}{\int_S (\bar{\lambda}_z)^2 ds}, \quad A_{zz}^{(n)} = 1 + \frac{e^4 \bar{A}_{66}}{144 \bar{A}_{55}^{(H)}} \frac{\int_S \left(\frac{dY}{ds}\right)^2 ds}{\int_S (\bar{\lambda}_y)^2 ds}, \tag{23a, b}$$

$$A_{\omega\omega}^{(n)} = 1 + \frac{e^4 \bar{A}_{66}}{144 \bar{A}_{55}^{(H)}} \frac{\int_S \left(\frac{\partial \omega_p}{\partial n}\right)^2 ds}{\int_S (\bar{\lambda}_\omega)^2 ds}, \quad A_{yz}^{(n)} = 1 + \frac{e^4 \bar{A}_{66}}{144 \bar{A}_{55}^{(H)}} \frac{\int_S \left(\frac{dY}{ds} \frac{dZ}{ds}\right) ds}{\int_S (\bar{\lambda}_y \bar{\lambda}_z) ds}, \tag{23c, d}$$

$$A_{y\omega}^{(n)} = 1 + \frac{e^4 \bar{A}_{66}}{144 \bar{A}_{55}^{(H)}} \frac{\int_S \left(\frac{\partial \omega_p}{\partial n} \frac{dZ}{ds}\right) ds}{\int_S (\bar{\lambda}_\omega \bar{\lambda}_z) ds}, \quad A_{z\omega}^{(n)} = 1 + \frac{e^4 \bar{A}_{66}}{144 \bar{A}_{55}^{(H)}} \frac{\int_S \left(\frac{dY}{ds} \frac{\partial \omega_p}{\partial n}\right) ds}{\int_S (\bar{\lambda}_y \bar{\lambda}_\omega) ds}. \tag{23e, f}$$

Another way to obtain equations (20a–e) is by substituting strain expressions (10) into constitutive equations (A.I.1) and there results into expressions (13).

On the other hand, this last approach for the constitutive equations corresponding to Q_y , Q_z and T_w leads to different expressions for the coefficients of matrix $[S]$. This occurs because expressions of N_{xs} and N_{xn} determined in this way do not verify the shell equilibrium equations (19). Consequently, expressions (20f) with equation (22) are more accurate than the constitutive expressions obtained in the form explained in the previous paragraph.

In order to clarify this point, it is interesting to consider the particular case of a plane Timoshenko beam vibrating in the $x-y$ plane. Expressions (20f) with (22) are reduced in this situation to the form

$$Q_y = 0.866GA \left(\frac{\partial v}{\partial x} - \theta_z \right), \tag{24a}$$

while the aforementioned second form leads to

$$Q_y = GA \left(\frac{\partial v}{\partial x} - \theta_z \right). \tag{24b}$$

It may be seen that the shear correction factor 0.866 arises naturally in expression (24a) but not in expression (24b). The present method of derivation based on the Hellinger–Reissner principle constitutes a generalization of an approach followed to obtain the Timoshenko’s beam theory developed in reference [22]

The present beam model is governed by equations (15) and (20) along with boundary conditions (16).

3. FREE VIBRATION AND BUCKLING ANALYSIS OF THIN-WALLED BEAMS WITH SIMPLY SUPPORTED ENDS

As it may be seen in governing equations (15), (16) and (20), the longitudinal motion is decoupled from the flexural–torsional motion. On the other hand, the governing equation corresponding to the axial motion has the classical form. Therefore, this case is not of interest. In what follows only the case of flexural–torsional motion is analyzed.

The beam is assumed to be simply supported at both ends. These boundary conditions are expressed in the form

$$v = w = \phi = 0, \quad E^* I_z \frac{\partial \theta_z}{\partial x} = E^* I_y \frac{\partial \theta_y}{\partial x} = E^* C_w \frac{\partial \theta}{\partial x} = 0 \quad \text{at } x = 0, L. \tag{25}$$

The previous boundary conditions are fulfilled by taking the following expressions for the generalized displacements:

$$v = \alpha_{1m} \sin\left(\frac{m\pi}{L}x\right)\beta_m(t), \quad w = \alpha_{3m} \sin\left(\frac{m\pi}{L}x\right)\beta_m(t), \quad \phi = \alpha_{5m} \sin\left(\frac{m\pi}{L}x\right)\beta_m(t), \tag{26a-c}$$

$$\theta_z = \alpha_{2m} \cos\left(\frac{m\pi}{L}x\right)\beta_m(t), \quad \theta_y = \alpha_{4m} \cos\left(\frac{m\pi}{L}x\right)\beta_m(t), \quad \theta = \alpha_{6m} \cos\left(\frac{m\pi}{L}x\right)\beta_m(t), \tag{26d-f}$$

where

$$\beta_m(t) = \cos[2\pi f_m t], \quad m = 1, 2, 3, \dots \tag{27}$$

the α_{im} ’s are constants and f_m is the frequency (Hz).

Substituting expressions (26) into equation (20) and then into equation (15), and factoring the trigonometric functions, the following algebraic system is obtained:

$$\sum_{j=1}^6 [K_{ij}^{(1)} + \lambda K_{ij}^{(2)} - (2\pi f_m)^2 M_{ij}] \alpha_{jm} = 0, \quad i = 1, \dots, 6, \tag{28}$$

where K_{ij}^1 , K_{ij}^2 and M_{ij} are symmetric matrices, whose expressions are displayed in Appendix B.

In equation (28), λ is a load factor defined by means of the expressions

$$N_{xx}^0 = \lambda \bar{N}_{xx}^0, \quad M_{xx}^0 = \lambda \bar{M}_{xx}^0, \tag{29}$$

where \bar{N}_{xx}^0 and \bar{M}_{xx}^0 are reference initial shell stress resultants, whose values are conveniently chosen.

The solution of the above eigenvalues problem yields the natural frequencies f_m . It is interesting to notice that there exist six frequencies for each value of m . On the other hand, the critical values of λ may be obtained from equation (28) by taking a zero value for the frequency f_m . The minimum value of λ corresponds to the buckling load.

4. NUMERICAL EXAMPLES AND DISCUSSION

To evaluate the shear effect on the dynamic and stability behavior of the analyzed structural members, numerical comparisons are performed among the present model predictions and results obtained by neglecting the shear deformability (Ghorbanpoor and Omidvar model). Different cross-sectional shapes, laminate schemes and slenderness ratios are considered. The analyzed material is graphite-epoxy (AS4/3501) whose properties are $E_1 = 144$ GPa, $E_2 = 9.65$ GPa, $G_{12} = 4.14$ GPa, $G_{13} = 4.14$ GPa, $G_{23} = 3.45$ GPa, $\nu_{12} = 0.3$, $\nu_{13} = 0.3$, $\nu_{23} = 0.5$, $\rho = 1389$ kg/m³. The considered laminate schemes are: (a) {0/0/0/0}, (b) {0/90/90/0} and (c) {45/-45/-45/45}. The analyzed cross-sections are shown in Figure 2.

4.1. VIBRATION PROBLEMS

In order to perform the numerical analyses, natural frequencies of vibration for the following situations are determined: flexural-torsional vibration of U beams— xz plane (Table 1); symmetric flexural vibration of U beams— xy plane- (Table 2); symmetric flexural vibration of rectangular section beams— xz plane (Table 3); symmetric flexural vibration of rectangular section beams— xy plane (Table 4); torsional vibration of rectangular section beams (Tables 5 and 7); torsional vibration of I beams (Tables 6 and 7); variation of the first frequency of the U beam versus an initial axial force N^0 (Figure 3); variation of the first frequency of the U beam versus an initial bending moment M_y^0 (Figure 4).

An examination of Tables 1–6 reveals that the general effect of the shear flexibility is to reduce the values of the natural frequencies in comparison with the frequencies obtained by means of the Ghoorbanpoor–Omidvar model. It is appreciated that the shear effect is very important for laminates (a) and (b), in fact when one of the principal axes of the

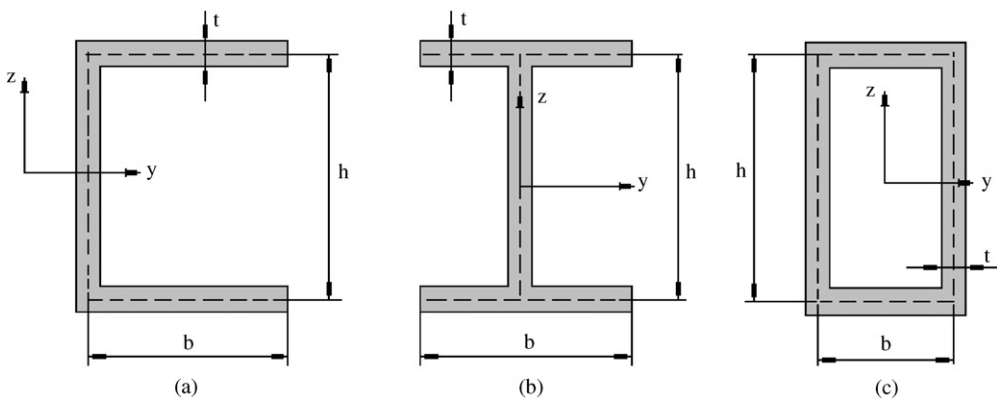


Figure 2. Analyzed cross-sectional shapes: (a) $b = h = 0.6$ m, (b) $b = h = 0.6$ m, (c) $b = h/2 = 0.3$ m; $t = 0.03$ m for all cases.

TABLE I

Flexural–torsional frequencies (Hz) of U beams —xz plane: [I] neglecting shear flexibility, [II] including shear flexibility, [III] percentage difference: $|100(f_{[III]}-f_{[I]})/f_{[I]}|$

Laminate	h/L	Model	f_1	f_2	f_3	f_4
{0/0/0/0}	0.05	[I]	9.82	38.63	52.07	86.64
		[II]	9.42	33.23	39.03	64.70
		[III]	(4.07)	(13.98)	(25.04)	(25.32)
	0.10	[I]	38.63	153.86	207.98	345.90
		[II]	33.23	99.03	102.79	169.05
		[III]	(13.98)	(35.64)	(50.58)	(51.13)
	0.15	[I]	86.64	345.90	467.84	777.95
		[II]	64.70	166.32	169.05	272.03
		[III]	(25.32)	(51.92)	(63.87)	(65.03)
{0/90/90/0}	0.05	[I]	7.30	28.35	38.09	63.41
		[II]	7.14	26.02	31.95	53.15
		[III]	(2.19)	(8.22)	(16.12)	(16.18)
	0.10	[I]	28.35	112.50	151.95	252.76
		[II]	26.02	84.94	93.02	153.81
		[III]	(8.22)	(24.50)	(38.78)	(39.15)
	0.15	[I]	63.41	252.76	341.73	568.31
		[II]	53.15	153.81	157.26	258.60
		[III]	(16.18)	(39.15)	(53.98)	(54.50)
{45/−45/−45/45}	0.05	[I]	5.34	15.53	18.45	31.32
		[II]	5.33	15.48	18.24	31.10
		[III]	(0.13)	(0.34)	(1.15)	(0.71)
	0.10	[I]	15.53	53.14	68.77	115.26
		[II]	15.48	52.50	65.76	112.22
		[III]	(0.34)	(1.22)	(4.37)	(2.63)
	0.15	[I]	31.32	115.26	152.67	254.84
		[II]	31.10	112.22	139.01	240.68
		[III]	(0.71)	(2.63)	(8.95)	(5.56)

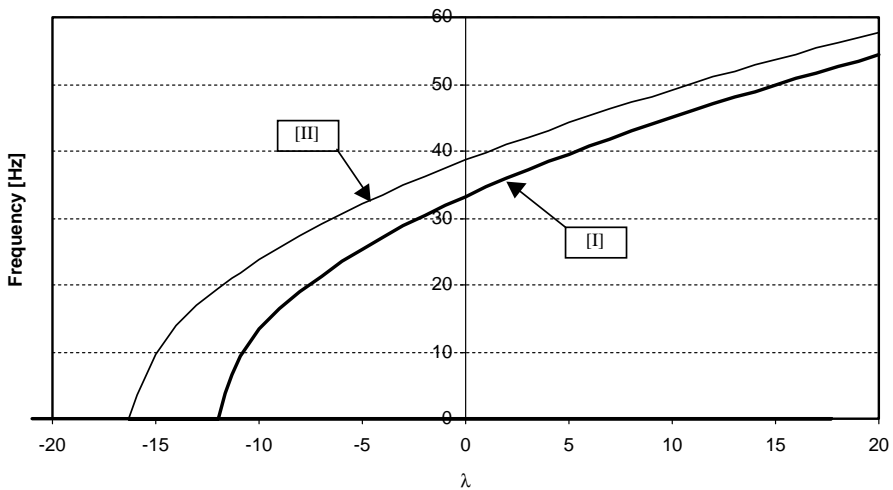


Figure 3. Variation of the first frequency (Hz) versus coefficient $\lambda = N^0/N_{ref}^0$; $N_{ref}^0 = 10^6$ N, $h/L = 0.10$, U beam, laminate {0/0/0/0}. [I] Considering shear flexibility, [II] neglecting shear flexibility.

TABLE 2

Flexural frequencies (Hz) of U beams—xy plane: [I] neglecting shear flexibility, [II] including shear flexibility, [III] percentage difference: $|100(f_{[III]}-f_{[I]})/f_{[I]}|$

Laminate	h/L	Model	f_1	f_2	f_3	f_4
{0/0/0/0}	0.05	[I]	22.21	88.85	199.92	355.42
		[II]	20.38	67.17	122.06	178.01
		[III]	(8.24)	(24.40)	(38.95)	(49.92)
	0.10	[I]	88.85	355.42	799.69	1421.67
		[II]	67.17	178.01	288.05	395.60
		[III]	(24.40)	(49.92)	(63.98)	(72.17)
	0.15	[I]	199.92	799.69	1799.30	3198.75
		[II]	122.06	288.05	448.76	606.77
		[III]	(38.95)	(63.98)	(75.06)	(81.03)
{0/90/90/0}	0.05	[I]	16.22	64.89	146.00	259.56
		[II]	15.46	54.75	105.76	160.85
		[III]	(4.69)	(15.63)	(27.56)	(38.03)
	0.10	[I]	64.89	259.56	584.01	1038.24
		[II]	54.75	160.85	272.53	382.40
		[III]	(15.63)	(38.03)	(53.33)	(63.17)
	0.15	[I]	146.00	584.01	1314.02	2336.04
		[II]	105.76	272.53	436.60	597.08
		[III]	(27.56)	(53.33)	(66.77)	(74.44)
{45/-45/-45/45}	0.05	[I]	7.18	28.70	64.58	114.82
		[II]	7.16	28.43	63.22	110.65
		[III]	(0.24)	(0.96)	(2.11)	(3.64)
	0.10	[I]	28.70	114.81	258.33	459.28
		[II]	28.43	110.64	238.88	403.69
		[III]	(0.96)	(3.63)	(7.53)	(12.10)
	0.15	[I]	64.58	258.33	581.24	1033.38
		[II]	63.22	238.88	496.99	809.59
		[III]	(2.11)	(7.53)	(14.49)	(21.66)

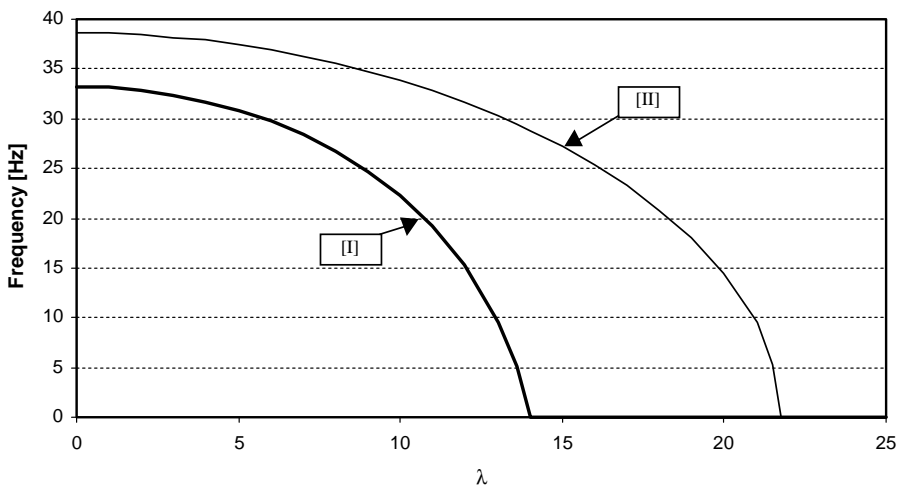


Figure 4. Variation of the first frequency (Hz) versus coefficient $\lambda = M_y^0/M_{y.ref}^0$: $M_{y.ref}^0 = 10^6$ N m, $h/L = 0.10$, U beam, laminate {0/0/0/0}. [I] Considering Shear flexibility, [II] Neglecting shear flexibility.

TABLE 3

Flexural frequencies (Hz) of rectangular section beams in the xz plane: [I] neglecting shear flexibility, [II] including shear flexibility, [III] percentage difference: $|100(f_{[II]} - f_{[I]})/f_{[I]}|$

Laminate	H/L	Model	f_1	f_2	f_3	f_4
{0/0/0/0}	0.05	[I]	24.84	99.34	223.52	397.37
		[II]	22.68	74.28	134.34	195.36
		[III]	(8.70)	(25.23)	(39.90)	(50.84)
	0.10	[I]	99.34	397.37	894.08	1589.47
		[II]	74.28	195.36	315.23	432.40
		[III]	(25.23)	(50.84)	(64.74)	(72.80)
	0.15	[I]	223.52	894.08	2011.67	3576.31
		[II]	134.34	315.23	490.34	662.59
		[III]	(39.90)	(64.74)	(75.63)	(81.47)
{0/90/90/0}	0.05	[I]	18.14	72.55	163.24	290.20
		[II]	17.24	60.75	116.80	177.04
		[III]	(4.96)	(16.26)	(28.45)	(38.99)
	0.10	[I]	72.55	290.20	652.94	1160.79
		[II]	60.75	177.04	298.80	418.49
		[III]	(16.26)	(38.99)	(54.24)	(63.95)
	0.15	[I]	163.24	652.94	1469.12	2611.77
		[II]	116.80	298.80	477.53	652.40
		[III]	(28.45)	(54.24)	(67.50)	(75.02)
{45/-45/-45/45}	0.05	[I]	8.02	32.08	72.17	128.32
		[II]	8.00	31.72	70.41	122.95
		[III]	(0.28)	(1.11)	(2.44)	(4.19)
	0.10	[I]	32.08	128.31	288.70	513.27
		[II]	31.72	122.94	263.93	443.28
		[III]	(1.11)	(4.18)	(8.58)	(13.64)
	0.15	[I]	72.17	288.70	649.57	1154.86
		[II]	70.41	263.93	544.08	878.87
		[III]	(2.44)	(8.58)	(16.24)	(23.90)

material coincides with the longitudinal axis of the beam. On the other hand, in the case of laminate (c), the shear effect is negligible. This behavior is due to the fact that beams with laminate (c) present a higher shear rigidity than beams with laminates (a) and (b). A way to show this fact is by considering the ratio G^*/E^* , which takes the values 0.03, 0.05 and 1 for cases (a), (b) and (c) respectively.

Tables 1–6 show that the shear effect increases with the increase of h/L (decrease of the slenderness of the beam) and with the increase of the mode number. It should be observed that, for the case of laminate (a), the shear effect is important even for the first frequency corresponding to slender beams. For example, in the case of the symmetric vibration of the U beam with $h/L = 0.05$, the decrease of the first frequency is 10%, approximately.

It is interesting to notice that the torsional modes of the rectangular section beams (Table 5) are practically unaffected by the shear flexibility. Differently, the torsional vibration of I beams is noticeably influenced by the shear effect. This discrepancy is due to the fact that, for the closed section, the torsional motion is governed by the Saint–Venant behavior (pure torsion), while for the open section case, the torsional motion is dominated by warping and therefore the shear warping is significant. The warping effect may be

TABLE 4

Flexural frequencies (Hz) of rectangular section beams in the xy plane: [I] neglecting shear flexibility, [II] including shear flexibility, [III] percentage difference: $|100(f_{[II]} - f_{[I]})/f_{[II]}|$

Laminate	H/L	Model	f_1	f_2	f_3	f_4
{0/0/0/0}	0.05	[I]	14.69	58.77	132.24	235.09
		[II]	13.48	44.42	80.67	117.60
		[III]	(8.24)	(24.42)	(39.00)	(49.98)
	0.10	[I]	58.77	235.09	528.94	940.34
		[II]	44.42	117.60	190.17	261.09
		[III]	(24.42)	(49.98)	(64.05)	(72.24)
	0.15	[I]	132.24	528.94	1190.12	2115.77
		[II]	80.67	190.17	296.14	400.34
		[III]	(38.99)	(64.05)	(75.12)	(81.08)
{0/90/90/0}	0.05	[I]	10.73	42.92	96.57	171.68
		[II]	10.23	36.24	70.00	106.41
		[III]	(4.69)	(15.55)	(27.51)	(38.02)
	0.10	[I]	42.92	171.68	386.29	686.73
		[II]	36.24	106.41	180.12	252.58
		[III]	(15.55)	(38.02)	(53.37)	(63.22)
	0.15	[I]	96.57	386.29	869.14	1545.14
		[II]	70.00	180.12	288.31	394.11
		[III]	(27.51)	(53.37)	(66.83)	(74.49)
{45/-45/-45/45}	0.05	[I]	4.75	18.99	42.73	75.98
		[II]	4.74	18.87	42.11	74.04
		[III]	(0.17)	(0.66)	(1.47)	(2.55)
	0.10	[I]	18.99	75.97	170.94	303.91
		[II]	18.87	74.03	161.68	276.72
		[III]	(0.66)	(2.55)	(5.42)	(8.95)
	0.15	[I]	42.73	170.94	384.61	683.79
		[II]	42.11	161.68	342.85	568.56
		[III]	(1.47)	(5.42)	(10.86)	(16.85)

appreciated in Table 7. This table shows torsional frequencies obtained by means of: (1) the present model, (2) the Vlasov's model, i.e. neglecting shear flexibility, and (3) the Saint-Venant model, i.e., neglecting shear and warping effects ($C_w = 0$). As it may be seen, for the closed section beam the warping effect is negligible. Conversely, for the I-section beam, this effect is very important.

From Figure 3, it is possible to appreciate that the effect of an axial compressive force is to decrease the fundamental frequency with respect to the unloaded case. Moreover, this decrease is more pronounced when the shear flexibility is included in the analysis. Similar observations can be established for the case of a beam pre-loaded with a bending moment as shown in Figure 4.

Figure 5 shows the first two modal shapes corresponding to the unloaded U beam with the cross-sectional characteristics reported in Figure 2 and with $h/L = 0.05$. It is interesting to note that the first modes corresponding to laminates (a) and (b) are dominated by torsion. In fact the ratio $(\phi)_{max}/(w)_{max}$ is of the order of 5. Differently, for the case of laminate (c) the behavior of the first mode has a flexural-torsional character. In this last case, the ratio $(\phi)_{max}/(w)_{max}$ takes a value of 1.4, approximately. The second

TABLE 5

Torsional frequencies (Hz) of rectangular section beams: [I] neglecting shear flexibility, [II] including shear flexibility, [III] percentage difference: $|100(f_{[III]} - f_{[I]})/f_{[III]}$

Laminate	h/L	Model	f_1	f_2	f_3	f_4
{0/0/0/0}	0.05	[I]	55.50	111.74	169.43	229.29
		[II]	55.49	111.60	168.60	226.43
		[III]	(0.02)	(0.13)	(0.49)	(1.25)
	0.10	[I]	111.74	229.29	357.99	502.39
		[II]	111.60	226.43	343.65	461.76
		[III]	(0.13)	(1.25)	(4.01)	(8.09)
	0.15	[I]	169.43	357.99	581.64	851.93
		[II]	168.60	343.65	520.91	698.31
		[III]	(0.49)	(4.01)	(10.44)	(18.03)
{0/90/90/0}	0.05	[I]	55.44	111.28	167.90	225.69
		[II]	55.44	111.23	167.60	224.63
		[III]	(0.00)	(0.04)	(0.18)	(0.47)
	0.10	[I]	111.28	225.69	346.22	475.60
		[II]	111.23	224.63	340.43	457.74
		[III]	(0.04)	(0.47)	(1.67)	(3.76)
	0.15	[I]	167.90	346.22	544.37	770.16
		[II]	167.60	340.43	516.69	694.00
		[III]	(0.18)	(1.67)	(5.08)	(9.89)
{45/-45/-45/45}	0.05	[I]	166.75	333.53	500.36	667.27
		[II]	166.74	333.47	500.17	666.84
		[III]	(0.01)	(0.02)	(0.04)	(0.06)
	0.10	[I]	333.53	667.27	1001.43	1336.22
		[II]	333.47	666.84	1000.02	1332.90
		[III]	(0.02)	(0.06)	(0.14)	(0.25)
	0.15	[I]	500.36	1001.43	1503.91	2008.52
		[II]	500.17	1000.02	1499.19	1997.34
		[III]	(0.04)	(0.14)	(0.31)	(0.56)

mode behavior is the same for all the laminates, from a qualitative point of view (Figure 6).

4.2. BUCKLING PROBLEMS

Critical values of λ are obtained for the cases of (I) an initial longitudinal force N^0 and (II) an initial bending moment M_y^0 . The adopted reference values are $N_{ref}^0 = -1 \times 10^6$ N and $M_{y_{ref}}^0 = 1 \times 10^6$ Nm respectively. Tables 8 and 9 show the values of $\lambda = N_{cr}^0/N_{ref}^0$ and $\lambda = M_{y_{cr}}^0/M_{y_{ref}}^0$, respectively, for the three types of cross-sectional shapes taken into account. In these tables, it is possible to observe that, for both situations and all the cross-sectional shapes, the shear effect is very important for laminates (a) and (b), while it is negligible for laminate (c). For example, in the case of laminate (a) when $h/L = 0.1$, the percentage differences of $\lambda = N_{cr}^0/N_{ref}^0$ among the present results and those obtained by neglecting the shear effect are 26, 25 and 43% for the U, I and rectangular sections respectively. On the other hand, the corresponding values for the case of laminate (c) are 2, 1 and 1%.

TABLE 6

Torsional frequencies (Hz) of I-beams: [I] neglecting shear flexibility, [II] including shear flexibility, [III] percentage difference: $|100(f_{[II]} - f_{[I]})/f_{[I]}|$

Laminate	h/L	Model	f_1	f_2	f_3	f_4
{0/0/0/0}	0.05	[I]	16.24	63.35	141.86	251.76
		[II]	15.64	55.00	107.55	165.41
		[III]	(3.69)	(13.18)	(24.19)	(34.30)
	0.10	[I]	63.35	251.76	565.78	1005.40
		[II]	55.00	165.41	284.29	401.86
		[III]	(13.18)	(34.30)	(49.75)	(60.03)
	0.15	[I]	141.86	565.78	1272.31	2261.46
		[II]	107.55	284.29	459.86	631.49
		[III]	(24.19)	(49.75)	(63.86)	(72.08)
{0/90/90/0}	0.05	[I]	12.19	46.61	103.95	184.21
		[II]	11.96	43.02	87.94	140.98
		[III]	(1.89)	(7.70)	(15.40)	(23.47)
	0.10	[I]	46.61	184.21	413.54	734.59
		[II]	43.02	140.98	257.02	375.94
		[III]	(7.70)	(23.47)	(37.85)	(48.82)
	0.15	[I]	103.95	413.54	929.52	1651.89
		[II]	87.94	257.02	435.12	610.43
		[III]	(15.40)	(37.85)	(53.19)	(63.05)
{45/-45/-45/45}	0.05	[I]	10.98	28.11	54.18	89.99
		[II]	10.96	27.98	53.61	88.35
		[III]	(0.15)	(0.49)	(1.05)	(1.83)
	0.10	[I]	28.11	89.99	191.65	333.74
		[II]	27.98	88.34	184.14	311.75
		[III]	(0.49)	(1.83)	(3.92)	(6.59)
	0.15	[I]	54.18	191.65	419.94	739.46
		[II]	53.61	184.14	386.03	644.07
		[III]	(1.05)	(3.92)	(8.07)	(12.90)

TABLE 7

Torsional frequencies (Hz) of rectangular and H section beams: [I] neglecting shear flexibility, [II] neglecting shear flexibility and warping, [III] including shear flexibility; material: graphite-epoxy 0/90/90/0, $h/L = 0.1$

Model	f_1	f_2	f_3	f_4
<i>H section</i>				
[I]	46.61	184.21	413.54	734.59
[II]	8.30	16.61	24.91	33.21
[III]	43.02	140.98	257.02	375.94
<i>Rectangular section</i>				
[I]	111.28	225.69	346.22	475.60
[II]	110.75	221.51	332.29	443.09
[III]	111.23	224.63	340.43	457.74

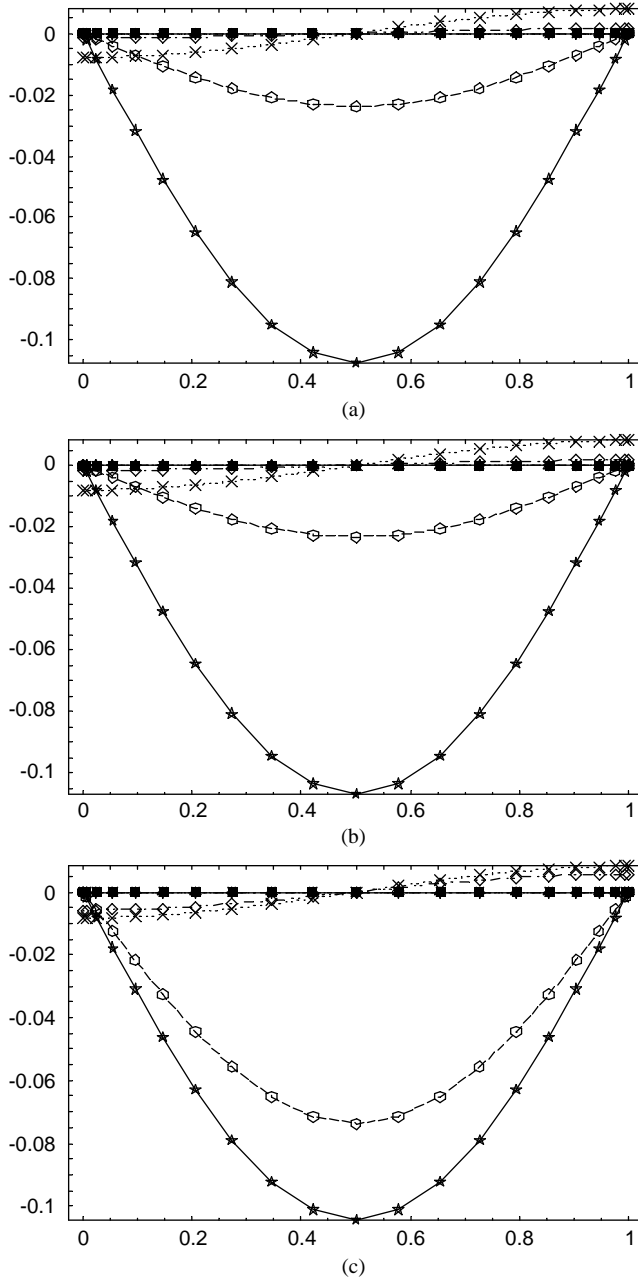


Figure 5. Mode shape corresponding to first frequency: (a) laminate $\{0/0/0/0\}$, (b) laminate $\{0/90/90/0\}$, (c) laminate $\{45/-45/-45/45\}$: \triangle , u_0 , \ast , v_1 , \blacksquare , θ_z ; \circ , w ; \diamond , θ_y ; \star , ϕ ; \times , θ .

5. CONCLUSIONS

- A theoretical model was developed for vibration analysis of composite thin-walled beams accounting for shear deformability.
- The theory is applicable to both open and closed cross-sections.

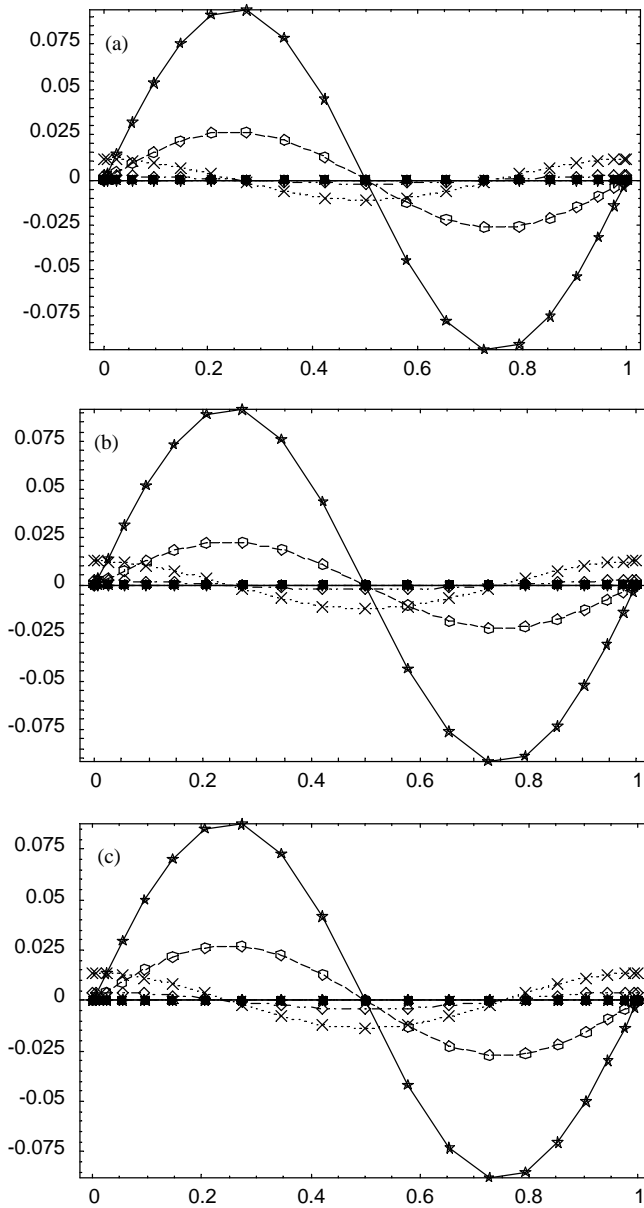


Figure 6. Mode shape corresponding to second frequency. (a) laminate $\{0/0/0/0\}$, (b) laminate $\{0/90/90/0\}$, (c) laminate $\{45/-45/-45/45\}$; \triangle , u_0 ; \star , v_t ; \blacksquare , θ_z ; \square , w ; \diamond , θ_y ; \star , ϕ ; \times , θ .

- The model considers the existence of initial shell stress resultants N_{xx}^0 and M_{xx}^0 . Therefore, it is possible to analyze buckling problems.
- The numerical results demonstrate that the shear flexibility has a remarkable effect on the natural frequencies and critical loads, especially when one of the material axes coincides with the longitudinal axis of the beam.
- The warping shear may be of great influence on the vibration and stability behavior for open section beams, although it is negligible for closed section beams.

TABLE 8

Coefficients $\lambda = N^0/N_{ref}^0$ of critical loading for point load at both ends: [I] neglecting shear flexibility, [II] including shear flexibility, [III] percentage difference: $|100(f_{[III]} - f_{[II]})/f_{[II]}|$

Laminate	h/L	Model	U profile	I profile	Rect. profile
{0/0/0/0}	0.05	[I]	4.16	10.67	9.33
		[II]	3.84	9.83	7.86
		[III]	(7.86)	(7.89)	(15.75)
	0.10	[I]	16.12	42.69	37.31
		[II]	11.94	31.79	21.34
		[III]	(25.89)	(25.53)	(42.79)
	0.15	[I]	36.04	96.05	83.94
		[II]	20.12	54.22	31.29
		[III]	(44.16)	(43.55)	(62.72)
{0/90/90/0}	0.05	[I]	2.30	5.69	4.97
		[II]	2.21	5.44	4.52
		[III]	(4.26)	(4.37)	(9.07)
	0.10	[I]	8.68	22.77	19.90
		[II]	7.32	19.25	14.22
		[III]	(15.61)	(15.46)	(28.51)
	0.15	[I]	19.30	51.23	44.77
		[II]	13.59	36.29	23.59
		[III]	(29.58)	(29.15)	(47.30)
{45/-45/-45/45}	0.05	[I]	1.23	1.11	0.97
		[II]	1.23	1.11	0.97
		[III]	(0.24)	(0.33)	(0.12)
	0.10	[I]	2.60	4.45	3.89
		[II]	2.59	4.32	3.86
		[III]	(0.38)	(2.92)	(0.74)
	0.15	[I]	4.71	10.01	8.75
		[II]	4.67	9.92	8.59
		[III]	(0.85)	(0.92)	(1.82)

It is interesting to point out that the shear effect may be even more important for other end conditions such as clamped-clamped in analogy with the isotropic case. A numerical study of this situation by means of a finite element based on the present theory is on course.

ACKNOWLEDGMENTS

The present study was sponsored by the Secretaría de Ciencia y Tecnología de la Universidad Tecnológica Nacional and by CONICET.

REFERENCES

1. E. J. BARBERO 1999 *Introduction to Composite Material Design*. London: Taylor & Francis Inc.
2. V. VLASOV 1961 *Thin Walled Elastic Beams*. Jerusalem: Israel Program for Scientific Translation.

TABLE 9

Coefficients $\lambda = M_y^0/M_{y\text{ref}}^0$ of critical loading for moments applied at both ends [I] neglecting shear flexibility, [II] including shear flexibility, [III] percentage difference: $|100(f_{\text{III}}-f_{\text{II}})/f_{\text{II}}|$

Laminate	h/L	Model	U profile	I profile	Rect. profile
{0/0/0/0}	0.05	[I]	5.54	3.31	9.15
		[II]	4.82	3.06	8.40
		[III]	(12.95)	(7.51)	(8.22)
	0.10	[I]	21.75	12.91	18.43
		[II]	13.60	9.69	13.92
		[III]	(37.48)	(24.96)	(24.44)
	0.15	[I]	48.78	28.91	27.94
		[II]	20.79	16.50	16.98
		[III]	(57.37)	(42.92)	(39.23)
{0/90/90/0}	0.05	[I]	3.01	1.81	6.68
		[II]	2.79	1.74	6.37
		[III]	(7.26)	(4.05)	(4.64)
	0.10	[I]	11.66	6.94	13.40
		[II]	8.84	5.90	11.33
		[III]	(24.21)	(14.98)	(15.48)
	0.15	[I]	26.08	15.47	20.22
		[II]	15.17	11.05	14.66
		[III]	(41.83)	(28.56)	(27.52)
{45/-45/-45/45}	0.05	[I]	1.07	0.72	8.86
		[II]	1.06	0.72	8.85
		[III]	(0.09)	(0.14)	(0.11)
	0.10	[I]	2.89	1.85	17.73
		[II]	2.87	1.84	17.65
		[III]	(0.69)	(0.54)	(0.45)
	0.15	[I]	5.75	3.56	26.60
		[II]	5.67	3.54	26.34
		[III]	(1.39)	(0.56)	(0.98)

- N. R. BAULD JR and L. S. TZENG 1984 *International Journal of Solids and Structures* **20**, 277–297. A Vlasov theory for fiber-reinforced beams with thin-walled open cross sections.
- A. GHORBANPOOR and B. OMIDVAR 1996 *Journal of Structural Engineering* **122**, 1379–1383. Simplified analysis of thin-walled composite members.
- J. C. MASSA and E. J. BARBERO 1998 *Journal of Composite Materials* **32**, 1560–1594. A strength of materials formulation for thin-walled composite beams with torsion.
- G. D. POLLOCK, A. R. ZAK, H. H. HILTON and M. F. AHMAD 1995 *Structural Engineering and Mechanics* **3**, 91–103. Shear center for elastic thin-walled composite beams.
- E. ESTIVALEZES and J.-J. BARRAU 1998 *Composites* **29B**, 371–376. Analytical theory for an approach calculation of composite box beams subjected to tension and bending.
- V. H. CORTÍNEZ and R. E. ROSSI 1998 *Revista Internacional de Métodos Numéricos para Cálculo y Diseño en Ingeniería* **14**, 293–316. Dynamics of shear deformable thin-walled open beams subjected to initial stresses (in spanish).
- V. H. CORTÍNEZ, M. T. PIOVAN and R. E. ROSSI 1999 *Structural Engineering and Mechanics* **8**, 257–272. Out-of-plane vibrations of thin-walled curved beams considering shear flexibility.
- V. H. CORTÍNEZ, M. T. PIOVAN and R. E. ROSSI 1999 *Journal of Sound and Vibration* **224**, 375–378. Comments on coupled flexural-torsional vibrations of Timoshenko beams.

11. A. N. SHERBOURNE and M. Z. KABIR 1995 *Journal of Engineering Mechanics* **121**, 640–647. Shear strains effects in lateral stability of thin-walled fibrous composite beams.
12. L. A. GODOY, E. J. BARBERO and I. RAFTOYIANNIS 1995 *Journal of Composite Materials* **29**, 591–613. Interactive buckling analysis of fiber-reinforced thin-walled columns.
13. B. OMIÐVAR 1996 *Journal of Composites for Construction* **2**, 46–56. Shear coefficient in orthotropic thin-walled composite beams.
14. E. C. SMITH and I. CHOPRA 1991 *Journal of the American Helicopter Society* **36**, 33–35. Formulation and evaluation of an analytical model for composite box-beams.
15. O. SONG and L. LIBRESCU 1993 *Journal of Sound and Vibration* **167**, 129–147. Free vibration of anisotropic composite thin-walled beams of closed cross-section contour.
16. O. SONG and L. LIBRESCU 1997 *Journal of the American Helicopter Society* **42**, 358–369. Structural modeling and free vibration analysis of rotating composite thin-walled beams.
17. O. SONG and L. LIBRESCU 1997 *Journal of Sound and Vibration* **204**, 495–504. Anisotropy and structural coupling on vibration and instability of spinning thin-walled beams.
18. K. BHASKAR and L. LIBRESCU 1995 *International Journal of Engineering Sciences* **33**, 1331–1344. A Geometrically non-linear theory for laminated anisotropic thin-walled beams.
19. X. X. WU and C. T. SUN 1990 *American Institute of Aeronautics and Astronautics Journal* **29**, 736–742. Vibration analysis of laminated composite thin-walled beams using finite elements.
20. K. WASHIZU 1968. *Variational Methods in Elasticity and Plasticity*. New York: Pergamon Press.
21. S. KRENK and O. GUNNESKOV 1981 *International Journal for Numerical Methods in Engineering* **17**, 1407–1426. Statics of thin-walled pretwisted beams.
22. V. H. CORTÍNEZ, M. T. PIOVAN and R. E. ROSSI 1999 *Structural Engineering and Mechanics* **7**, 527–530. A Consistent derivation of the Timoshenko's beam theory.

APPENDIX A: CONSTITUTIVE EQUATIONS OF SYMMETRICALLY BALANCED LAMINATES

The constitutive equations of symmetrically balanced laminates may be expressed in terms of shell stress resultants in the following form [1]:

$$\begin{pmatrix} N_{xx} \\ N_{xs} \\ N_{xn} \\ M_{xx} \\ M_{xs} \end{pmatrix} = \begin{bmatrix} \bar{A}_{11} & 0 & 0 & 0 & 0 \\ 0 & \bar{A}_{66} & 0 & 0 & 0 \\ 0 & 0 & \bar{A}_{55}^{(H)} & 0 & 0 \\ 0 & 0 & 0 & \bar{D}_{11} & 0 \\ 0 & 0 & 0 & 0 & \bar{D}_{66} \end{bmatrix} \begin{pmatrix} \varepsilon_{xx}^L \\ \gamma_{xs}^L \\ \gamma_{xn}^L \\ \kappa_{xx}^L \\ \kappa_{xs}^L \end{pmatrix} \quad (\text{A.1})$$

with

$$\bar{A}_{11} = A_{11} - \frac{A_{12}^2}{A_{22}}, \quad \bar{A}_{66} = A_{66} - \frac{A_{26}^2}{A_{22}}, \quad \bar{A}_{55}^{(H)} = A_{55}^{(H)} - \frac{(A_{45}^{(H)})^2}{A_{44}^{(H)}}, \quad (\text{A.2a-c})$$

$$\bar{D}_{11} = D_{11} - \frac{D_{12}^2}{D_{22}}, \quad \bar{D}_{66} = D_{66} - \frac{D_{26}^2}{D_{22}}, \quad (\text{A.2d, e})$$

where A_{ij} , D_{ij} and $A_{ij}^{(H)}$ are plate stiffness coefficients defined according to the lamination theory presented in reference [1, Chapter 6]. The coefficient \bar{D}_{16} has been neglected because of its low value for the considered laminate stacking sequence.

APPENDIX B: MATRIX ELEMENTS

Elements of matrix equation (28) are

$$\begin{aligned}
 K_{11}^{(1)} &= G^* S_{yy} \Gamma_n^2, & K_{12}^{(1)} &= -G^* S_{yy} \Gamma_n, & K_{13}^{(1)} &= G^* S_{yz} \Gamma_n^2, \\
 K_{14}^{(1)} &= -G^* S_{yz} \Gamma_n, & K_{15}^{(1)} &= G^* S_{y\omega} \Gamma_n^2, & K_{16}^{(1)} &= -G^* S_{y\omega} \Gamma_n, \\
 K_{22}^{(1)} &= G^* S_{yy} + E^* I_z \Gamma_n^2, & K_{23}^{(1)} &= -G^* S_{yz} \Gamma_n, & K_{24}^{(1)} &= G^* S_{yz}, \\
 K_{25}^{(1)} &= -G^* S_{y\omega} \Gamma_n, & K_{26}^{(1)} &= G^* S_{y\omega}, & K_{33}^{(1)} &= G^* S_{zz} \Gamma_n^2, \\
 K_{34}^{(1)} &= -G^* S_{zz} \Gamma_n, & K_{35}^{(1)} &= G^* S_{z\omega} \Gamma_n^2, & K_{36}^{(1)} &= -G^* S_{z\omega} \Gamma_n, \\
 K_{44}^{(1)} &= G^* S_{zz} + E^* I_y \Gamma_n^2, & K_{45}^{(1)} &= -G^* S_{z\omega} \Gamma_n, & K_{46}^{(1)} &= G^* S_{z\omega}, \\
 K_{55}^{(1)} &= (G^* S_{\omega\omega} + G^{**} J) \Gamma_n^2, & K_{56}^{(1)} &= -G^* S_{\omega\omega} \Gamma_n, \\
 K_{66}^{(1)} &= G^* S_{\omega\omega} + E^* C_w \Gamma_n^2, & K_{11}^{(2)} &= N^0 \Gamma_n^2, & K_{33}^{(2)} &= N^0 \Gamma_n^2,
 \end{aligned}$$

$$\begin{aligned}
 K_{55}^{(2)} &= (N^0 I_s / A + \beta_w B^0 + \beta_y M_y^0 + \beta_z M_z^0) \Gamma_n^2, & K_{35}^{(2)} &= (N^0 y_0 + M_z^0) \Gamma_n^2, \\
 K_{25}^{(2)} &= -(N^0 z_0 + M_y^0) \Gamma_n^2,
 \end{aligned}$$

$$\begin{aligned}
 M_{11} &= M_{33} = \bar{\rho} A, & M_{15} &= -\bar{\rho} A z_0, & M_{35} &= \bar{\rho} A y_0, & M_{22} &= \bar{\rho} I_z, \\
 M_{44} &= \bar{\rho} I_y, & M_{55} &= \bar{\rho} I_s, & M_{66} &= \bar{\rho} C_w,
 \end{aligned}$$

$$\begin{aligned}
 M_{12} &= M_{13} = M_{14} = M_{16} = M_{23} = M_{24} = M_{25} = M_{26} = M_{34} = M_{36} = M_{45} \\
 &= M_{46} = M_{56} = 0,
 \end{aligned}$$

where $\Gamma_n = n\pi/L$, and $K_{ji}^{(k)} = K_{ij}^{(k)}$, $k = 1, 2$ and $i, j = 1, \dots, 6$.